

Investigating the effect of changing the structural parameters of capacitive sensors on their response to the humidity of steam

Du Lipeng, Zhang Wenchao

Energy Resource and Power Engineering College, Northeast Dianli University, Jilin, Jilin, 132012

ad186062@163.com

Keywords: steam humidity; structural parameters; capacitive sensor; response characteristics.

Abstract. According to basic electromagnetic theory, the response of a capacitive sensor depends on the structural parameters of the sensor and the dielectric permittivity between the plates. Here, the effect on the response of a capacitive sensor is investigated by changing its structural parameters. In the experiments, a nozzle is used to make wet steam and to control its humidity. A heating method is used to calibrate humidity of the steam. A Schmitt oscillation circuit is used to measure the capacitance of the sensors. Three sensors with different structural parameters are investigated. The standard $k-\epsilon$ turbulence model, the wall function and the Semi-Implicit Method for Pressure Linked Equations (SIMPLE) algorithm are used to simulate the coupled performance of the electric field and the flow field in different structured sensors. There was a linear relationship with the humidity of the steam and the capacitance of the humidity sensor decreased with an increasing plate thickness. The capacitance change ratio was dependent on the humidity of the steam and increased with an increasing plate length. The capacitance change ratio decreased with an increasing plate separation. The stability and error of the sensors increased as the ratio between the plate length and plate separation increased. The linear relationship between the capacitance of the sensors and the steam humidity increased initially and then decreased as the ratio between the plate length and plate separation increased..

Introduction

Accurately measuring the humidity of steam is important to the economy and the security of steam turbines and nuclear power systems. Accurately measuring the humidity of steam is still a problem around the world. A tracer method is used to measure the humidity of steam in nuclear power plants, which has high measurement accuracy. However, the equipment is expensive and its operation is complicated (Lanford et al., 1976; Council et al, 1979; Luijtana, et al, 1998; Chen et al, 1978, Wang, 2005, Lovelock, 2001, Tian et al, 2005).

Capacitive sensors have the advantages of high temperature stability, simple structures, good adaptability and sensitive dynamic responses. They are also inexpensive and can be used for non-contact measurements (Ning, 2007). Based on the theory of dielectrics, the use of capacitive sensors to measure the humidity of steam has been investigated (Ning, 2006 , Kang and Kensall,2007). The structural parameters are important for the capacitive sensing response. Gregory and Scott (Gregory and Mattar, 1973), Abouelwafa and Kendall (1979, 1980) and Borst (1983) studied the performance of capacitive sensors with different structured electrodes. Their results showed the performance of capacitive sensors with spiraling electrodes. Kendoush (1995) studied the performance of five types of capacitive sensors with different structured electrodes and showed how changing the adjacent plates affected the static errors of the sensors.

Yu et al. (2004) studied a square capacitance sensor which consisted of 16 measurement electrodes to heighten the sensitivity of the sensor. On the basis of a theoretical analysis, a mathematical model of the capacitance was built. According to the variation principle, the finite element model (FEM) of the system was established by changing the finite boundary value problem of electrical capacitance tomography (ECT) into an equivalence variation problem, the capacitance field sensitivity distribution finite element was set up and its FEM software was programmed using the FEM of the system. The FEM program was then used to numerically simulate the square capacitance sensor. Comparison of the simulation results with the static experimental results shows that the error between

them is less than 1%. The optimization of the structural parameters of the capacitance sensor was proposed and the capabilities of the capacitance sensor were improved.

Delfo and Whitaker (2001) developed the averaged volume from the frequency-dependent governing equations for electrohydrodynamics. The authors determined that a single-equation model describing the coupled transport of the momentum and the electric charge could be obtained when the concept of the local electrical equilibrium was identified. Separate forms of Maxwell's equations must be developed for both the fluid and the solid phases, when the local electrical equilibrium is not valid.

Du (2011, 2012, 2013) developed a program to compute the electric field in FLUENT UDF code and it was used to numerically simulate the coupling of the electric field and the steam flow field within capacitance sensors. The result shows that the maximum difference between the experimental data and the numerical simulation data is 0.78 nF, which is a discrepancy of 19.8%.

In this paper, the effect of the capacitive sensor's response is studied by changing its structural parameters. The response is investigated using both experimental and numerical methods, and a program to compute the electric field in FLUENT UDF code was compiled in this investigation.

Principle of Capacitance Sensors for Measuring the Humidity of Steam

According to electromagnetism, the capacitance of a capacitor is determined by its geometry, the relative location of the electrode plates and the permittivity of the dielectric medium. The relationship is expressed as:

$$C = f(\varepsilon, S, \delta) \quad (1)$$

where C is the capacitance, ε is the permittivity, S is the area of overlap of the two electrode plates and δ is the distance between the electrode plates.

Thermally Measuring the Humidity of Wet Steam with Capacitive Sensors

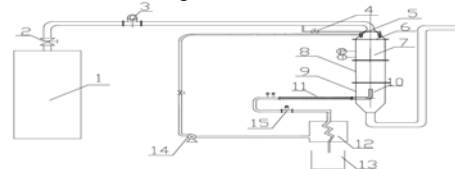
Experimental Set up

Thermal experiments were used to measure the humidity of steam with capacitive sensors. The effect of the structural parameters on the performance of capacitive sensors was investigated. The capacitance and experimental set up are shown in Figure 1. The steam was produced by boiling water and flowing the vapor through a variable diameter, a mixing region, a steam sampling region and finally directly into the atmosphere. In the experimental set up, the humidity of the steam was changed by a spraying system. The humidity of the steam was calibrated by heating it. The capacitance of the capacitive sensor was converted to a frequency signal by a Schmidt oscillation circuit. An oscilloscope and a frequency counter were used to collect the data.



1–fixed bracket, 2–flange, 3–inner electrode plate, 4–outermost electrode plate and 5–wire.

A. Capacitive sensor.



1–boiler, 2–valve, 3–flow meter, 4–valve, 5–spraying system, 6–variable diameter, 7–mixing region, 8–experimental region, 9–sampling region, 10–steam sampling probe, 11–heating region, 12–condenser, 13–water gatherer, 14–pump, and 15–flow meter.

B Experimental set up

Figure 1. (A) The capacitive sensor and (B) the experimental set up used to measure the humidity of steam with a capacitance method.

Experimental data processing

(1) Calibration of the steam humidity

The humidity of the steam was calibrated by heating it. The wet steam was heated to a superheated state, according to the principle of heat balance. The steam parameters were applied before and after heating to calculate the humidity of the steam using:

$$Y = \frac{W - W_s}{m(h_1'' - h_1')} + \frac{h_2 - h_1''}{h_1'' - h_1'} \quad (2)$$

where Y is the humidity of the steam; m is the mass flow of the steam in kg/s; W and W_s are the actual heat flux and the heat loss in kJ, respectively; h_1'' , h_1' , h_2 are the specific enthalpy of the dry saturated steam, the saturated water under the pressure of the heating pipe inlet and the steam at the exit of the heating pipe in J/kg, respectively.

(2) Measuring the capacitance of the sensors

The frequency of the Schmidt oscillation circuit and the capacitances of capacitive sensors were measured using:

$$C = \frac{12.99 \times 10^4}{f} \quad (3)$$

where f is the frequency of the Schmidt oscillation circuit and C is the capacitance of the capacitive sensor.

(3) Error analysis for the capacitance sensor

The errors for the capacitive sensors include: non-linear errors, random repeat errors and hysteresis errors.

① Non-linear errors

The expression for the non-linear errors is:

$$\xi_L = \frac{|\Delta y_L|_{\max}}{y_{FS}} \times 100\% \quad (4)$$

where y_{FS} is the full-scale output of the sensor and $(\Delta y_L)_{\max}$ is the maximum value of the measured data.

② Random repeat errors

The range method could be used to calculate the standard error of the measurement at point j , using the expressions:

$$s_{uj} = \frac{W_{uj}}{d_m} \quad (5)$$

$$W_{uj} = \max(y_{uji}) - \min(y_{uji}) \quad (6)$$

where W_{uj} is the range, d_m is the coefficient that depends on the measuring time m , y_{uji} is the value at point j for a measuring time of i .

Equation (6) is the expression for the repeatability. The standard error (s) is used for the random errors in the sensor. The expression for the random repeat errors is:

$$s = \max(s_{uj}) \quad (7)$$

$$\xi_R = \frac{3s}{y_{FS}} \times 100\% \quad (8)$$

where ξ_R is the random repeat error.

③ Hysteresis errors

The error measured at point j , measured n times can be calculated using equation (9).

$$\Delta C = |C_{ji} - C_{jk}| \quad (i \text{ and } k=1,2,3) \quad (9)$$

The hysteresis index can be calculated using equation (10).

$$\Delta C_{\max} = \max(\Delta C) \quad (i \text{ and } k=1,2,3) \quad (10)$$

The hysteresis errors can be calculated using equation (11).

$$\xi_H = \frac{\Delta C_{\max}}{2y_{FS}} \times 100\% \quad (11)$$

The error for the capacitance sensor is given by:

$$\xi_a = \sqrt{\xi_L^2 + \xi_H^2 + \xi_R^2} \quad (12)$$

Effect of the ratio between the plate length and the plate separation on the response of the sensors.

It is known that the plate length and plate separation in capacitors are important parameters. Three capacitive sensors were fabricated to investigate the effect of the ratio between the plate length and the plate separation on the response performance of the sensors. The sensors are called: sensor A, sensor B and sensor C, and the ratios between the plate length and plate separation were $(lct/d)_A=100$, $(lct/d)_B=50$ and $(lct/d)_C=33.3$, respectively.

Stability of the sensors

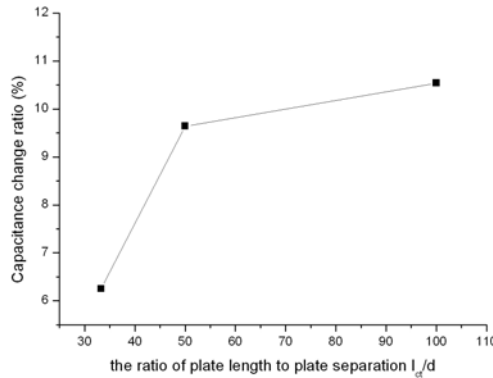


Figure 2. Capacitance change ratio vs the ratio between the plate length and plate separation.

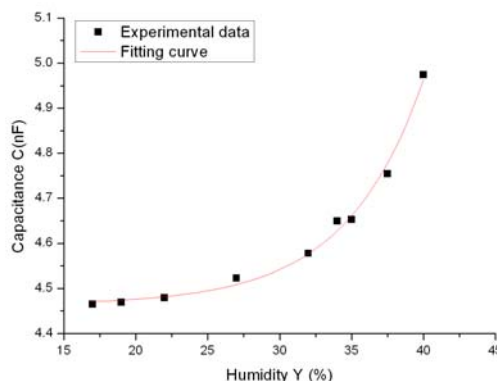


Figure 3. Capacitance of sensor A vs the humidity of steam.

The experimental results show that the capacitance of the sensors drifted with time. The capacitance change ratios were 10.54, 9.64 and 6.25%, for capacitors A, B and C, respectively. Figure 2 shows that the capacitance change ratio increased when the plate length/separation ratio increased. The data also show that the stability of the sensor decreased when plate length/separation ratio increased.

Effect on the relationship between the capacitance of the sensor and the humidity of steam

Figure 3 shows that the relationship between the capacitance of sensor A and the humidity of steam is exponential.

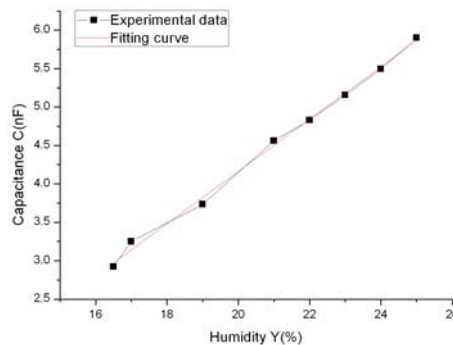


Figure 4. Capacitance of sensor B vs the humidity of steam.

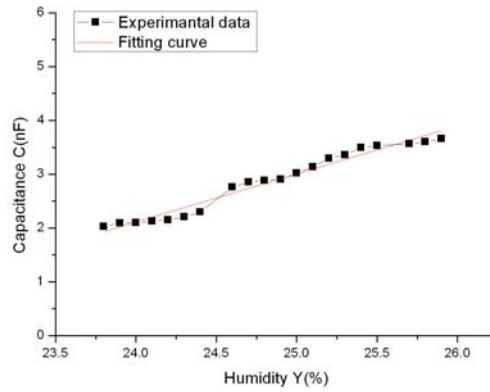


Figure 5. Capacitance of sensor C vs the humidity of steam.

Figures 4 and 5 show that the relationships between the capacitance of sensors and the steam humidity is linear. According to the experimental data, the linearity of sensors B and C could be calculated by Eq. (4), giving $\xi_L^B = 7.9\%$ and $\xi_L^C = 9.2\%$. This result shows that the linearity of the capacitive sensors increased initially and then decreased when the plate length/separation ratio increased.

Sensitivity of the sensors

According to the experimental data, the sensitivity of the sensors was not fixed, but fluctuated around a fixed value. The average sensitivity and the change in the sensitivity ratios for sensors A, B and C are shown in Figures 6 and 7. The average sensitivity values are 1.65 nF/%, 0.82 nF/% and 0.8 nF/%, respectively and the changes in the sensitivity ratios are 21.9, 11.2 and 16.5%, respectively. These results show that the sensitivity and sensitivity stability both increased initially and then decreased when the plate length/separation ratio increased.

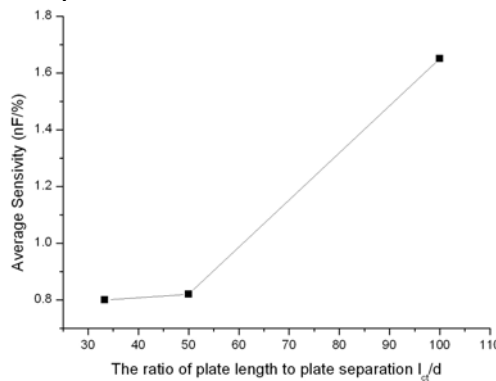


Figure 6. Capacitance sensitivity vs the plate length/separation ratio.

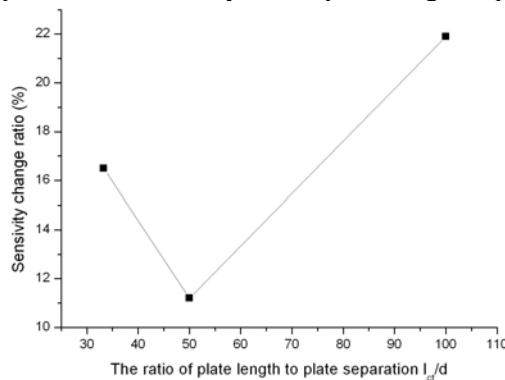


Figure 7. Change in the ratio of the capacitance sensitivity vs the plate length/separation ratio.

Effect of errors in the sensors

The linear relationship between the capacitance and the humidity of steam for sensor A was the worst. Thus, the errors in sensor A were the biggest. The errors in sensors B and C were calculated using equation (11), giving $\zeta_{aB} = 18.3\%$ and $\zeta_{aC} = 15.6\%$, respectively.

These results show that the errors in the sensors increased when the plate length/separation ratio increased.

Numerical Simulations

Physical model and control equations

There was an electric field and a steam flow field in the capacitive sensors as the steam flowed through them. The control equations are electrostatics and hydrodynamic equations. The principle of dielectric polarization is complicated. For the coupled numerical simulations on the electric field and the steam flow field it was assumed that: (1) the steam in the sensor was viscous and saturated, (2) the steam flow rate was steady, (3) the polarization was uniform, (4) the applied electric field was static and (5) the rate of change of the permittivity varied linearly with the humidity. The control equations are:

$$\nabla \cdot (\nabla U) = -\frac{\rho(\eta)}{\varepsilon} \quad (13)$$

$$\frac{\partial \rho(\eta)}{\partial t} + \nabla \cdot [(K \vec{E} + \vec{V}) \rho(\eta)] = 0 \quad (14)$$

$$\frac{\partial \rho}{\partial t} + \nabla \cdot (\rho \vec{V}) = 0 \quad (15)$$

$$\frac{\partial (\rho \vec{V})}{\partial t} + \nabla \cdot (\rho \vec{V} \vec{V}) = -\nabla p + \mu \nabla \cdot (\nabla \vec{V}) + \frac{1}{3} \mu \nabla (\nabla \cdot \vec{V}) + \vec{E} \rho(\eta) \quad (16)$$

where E is the intensity of the electric field in N/C; $\rho(\eta)$ is the density of charges in C/m³; ε is the permittivity; V is the voltage in V; \vec{V} is the velocity in m/s; ρ is the density in kg/m³; p is the pressure in Pa; and μ is the dynamic viscosity in m²/s.

Turbulence model and boundary conditions

(1) Turbulence model

The standard $k-\varepsilon$ model was applied. The wall function was used near the wall boundary. The equation for this is given in the literature [8].

(2) Boundary conditions

The boundary conditions include the hydrodynamic boundary conditions and electrostatics boundary conditions.

1) Hydrodynamic boundary conditions

- ① Inlet: the mass flow of the inlet was given.
- ② Outlet: the pressure of the outlet was 1 atm.
- ③ Wall: the electrode plate of the sensor was adiabatic and there was no slipping.

2) Electrostatics boundary conditions

- ① The voltage of the sensor was given and the potential of the negative plate was zero.
- ② The voltages of the inlet and outlet were both zero.

Analysis of the sensitivity of the mesh

The electric field and flow field in the capacitive sensors whose plate thickness was ignored initially were numerically simulated with the FLUENT software and User Defined Function (UDF) programs. To determine a suitable mesh, the numerical simulations were carried out four times with different meshes. The numbers of cells were 850,000, 1,200,000, 1,800,000 and 2,400,000, for Y+ values of 0.98, 1.23, 3.42 and 5.81, respectively. The mesh is shown in Figure 8.

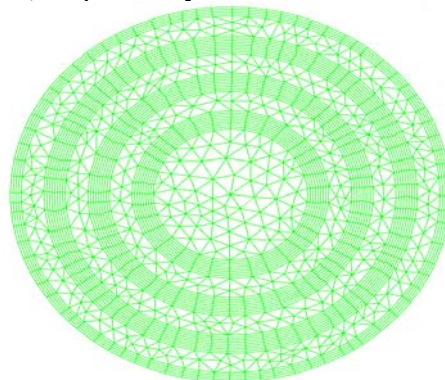


Figure 8. Structure of the mesh in a capacitance sensor.

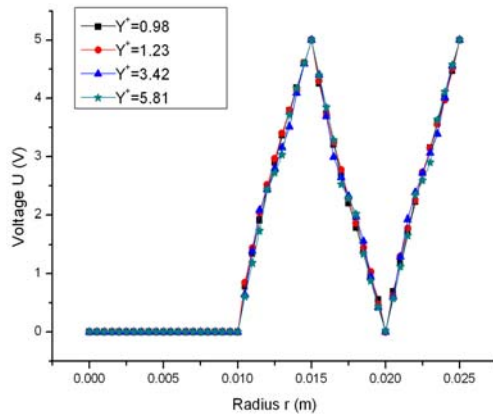


Figure 9. Voltage vs the radius for different meshes in the same section.

The simulation results for different meshes are shown in Figures 9 and 10. Figure 9 shows that the voltage did not depend on the mesh and the effect of the frame of the mesh on the voltage was ignored. Figure 10 shows that the velocity of the steam depends on the mesh and the effect of the frame of the mesh on the velocity cannot be ignored. The difference in the velocity between the plates was minimal for the meshes with $Y^+=0.98$ and $Y^+=1.23$. However, the difference in the velocity inside the inner most plate was minimal for the meshes with $Y^+=1.23$ and $Y^+=5.81$. Thus, the mesh with $Y^+=1.23$ cells was chosen.

Effect of Changing the Structural Parameters on the Sensor's Response

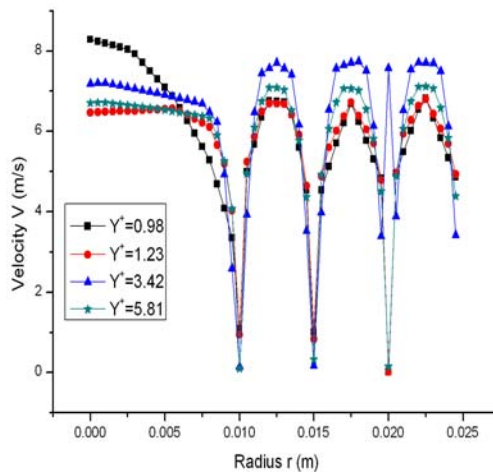


Figure 10. Velocity vs the mesh radius for different meshes in the same section.

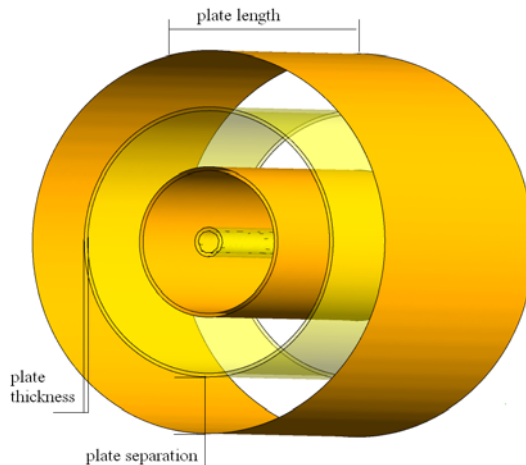


Figure 11. Structure of the simulated capacitance sensor

The structure of the sensors investigated is shown in Figure 11, where the plate thickness, plate length and plate separation are important parameters.

Comparison of the experimental and numerical simulation results

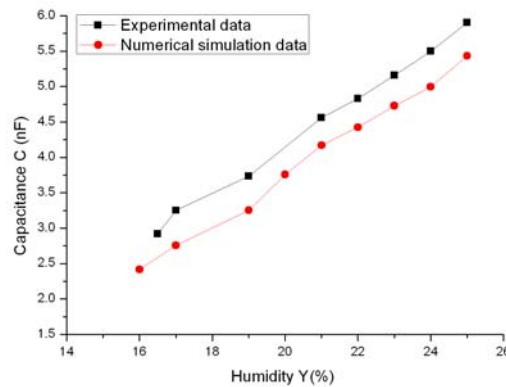


Figure 12. Capacitance of sensor B vs the humidity of steam.

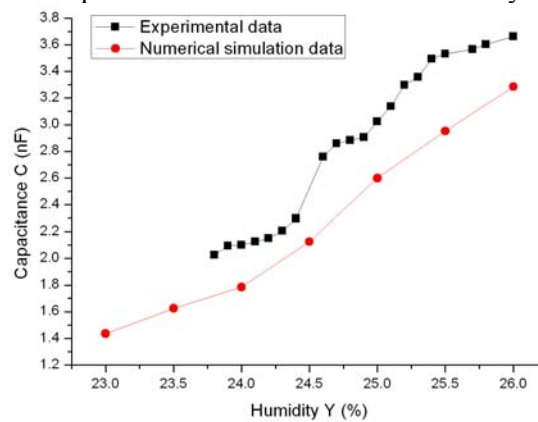


Figure 13. Capacitance of sensor C vs the humidity of steam.

Figures 12 and 13 show the capacitance versus steam humidity for the simulations and experiments. The numerical simulation results differ from the experimental results, but the trends of the output capacitance were the same. The capacitance increased linearly with increasing humidity. The maximum errors for sensors B and C for the experiments and numerical simulations were 13.9 and 19.8%, respectively.

Effect of the plate thickness

The plate thickness is one of the important parameters in capacitance sensors. Sensors with different plate thicknesses were investigated using numerical simulations. The plate thicknesses were $l_b=1$ mm, $l_b=1.5$ mm, $l_b=2$ mm and $l_b=3$ mm.

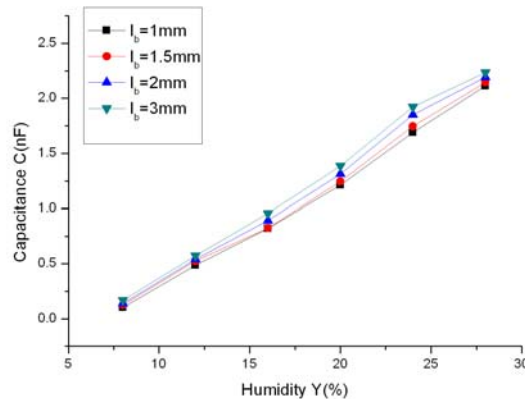


Figure 14. Capacitance of sensors with different plate thickness vs the humidity of steam.

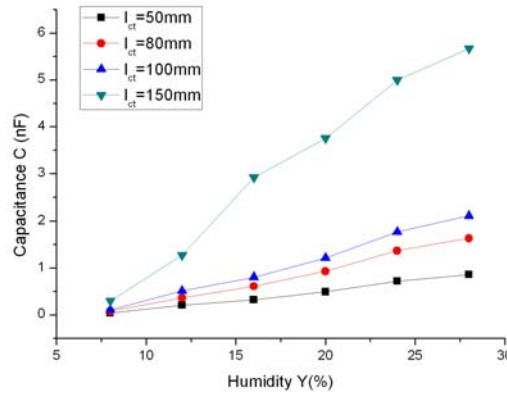


Figure 15. Capacitance of sensors with different plate lengths vs the humidity of steam.

Figure 14 shows the relationship between the capacitances of sensors with different plate thickness and steam humidity values. It is known that the capacitance of a sensor increases with increasing steam humidity. The relationship between the sensor capacitance and steam humidity is linear. If the steam humidity was constant, the capacitances of the sensors increased with an increasing plate thickness. The mean square error of the linear fitting expression for the capacitances of the sensors and the humidity of the steam were $R_{l_b=1\text{mm}}=0.99582$, $R_{l_b=1.5\text{mm}}=0.99579$, $R_{l_b=2\text{mm}}=0.99547$ and $R_{l_b=3\text{mm}}=0.99419$. This shows that the linear relationship between the capacitance of the sensor and the humidity of steam increased with a decreasing plate thickness. This occurred because the edge effects decreased with a decreasing plate thickness.

Effect of the plate length

The plate length is also an important parameter for capacitance sensors. Sensors with different plate lengths were investigated with numerical simulations. The plate used lengths were $l_{ct}=50$ mm, $l_{ct}=80$ mm, $l_{ct}=100$ mm and $l_{ct}=150$ mm.

Figure 15 shows the relationship between the capacitances of sensors with different plate lengths and steam humidity values. It is known that the relationship between the capacitance of a sensor and the humidity of steam is linear. If the humidity of steam was constant, the capacitance of the sensors increased with an increasing plate length. If the change in the plate length was constant, the capacitance of the sensor increased with an increasing plate length. If the humidity of the steam was constant, the capacitance change ratio increased with an increasing plate length.

Effect of the plate separation

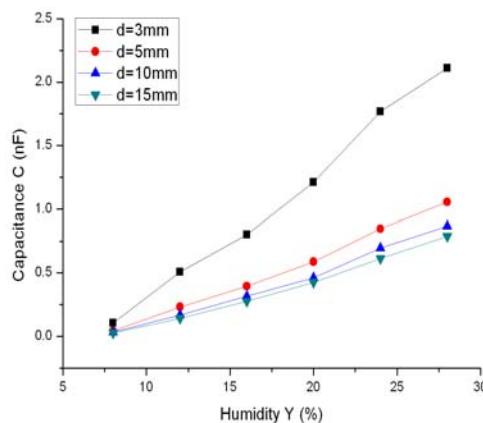


Figure 16. Capacitance of the sensors with different plate separations vs the humidity of steam.

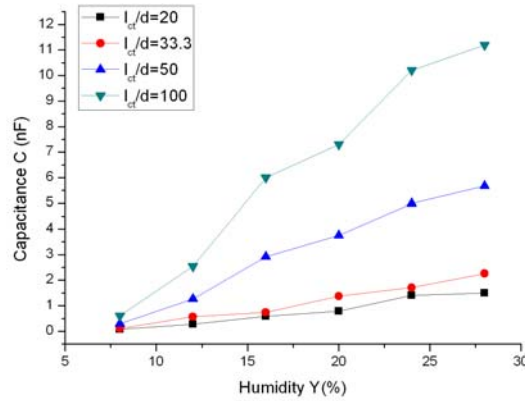


Figure 17. Capacitance of sensors with different plate length/separation ratios vs the humidity of steam.

Sensors with different plate separations were investigated. The plate separations used were $d=3$ mm, $d=5$ mm, $d=10$ mm and $d=15$ mm. Figure 16 shows the relationship between the capacitance of a sensor with different plate lengths and humidity values for the steam.

It is known that the capacitance of a sensor decreases with an increasing plate separation if the steam humidity is constant. If the plate separation is constant, the capacitance of the sensor decreases with an increasing plate separation. If the steam humidity is constant, the capacitance change ratio decreases with an increasing plate separation.

Effect of the ratio between the plate length and the plate separation

Sensors with different plate length/separation ratios were investigated. The ratios used were 20, 33.3, 50 and 100. Figure 17 shows the relationship between the capacitances for sensors with different plate length/plate separation ratios.

It is known that the capacitance of a sensor increases with an increasing plate length/separation ratio when the steam humidity kept constant. The mean square error of the linear fitting expression for the capacitances of sensors and the steam humidity were $R_{l_{ct}/d=20}=0.989$, $R_{l_{ct}/d=33.3}=0.990$, $R_{l_{ct}/d=50}=0.991$ and $R_{l_{ct}/d=100}=0.976$. It is known that the linearity of a sensor with a plate length/separation ratio of 50 is optimal. This result shows that the linearity of a capacitive sensor increased initially and then decreased when the ratio between the plate length and plate separation increased. This agrees with the experimental results.

Conclusions

The effect of changing the structural parameters on the response of capacitance sensors was investigated using experiments and numerical simulations. The conclusions are: (1) The linear relationship between the capacitance of a sensor and the humidity of steam increased with a decreasing plate thickness. (2) If the humidity of the steam was constant, the capacitance of the sensors increased with an increasing plate length. The capacitance change ratio of the sensor increased with an increasing plate length. If the humidity of the steam was kept constant, the capacitance change ratios increased with an increasing plate length. (3) The capacitances of the sensors decreased when the plate separation was increased and the steam humidity was constant. The capacitance change ratio of the sensor decreased with an increasing plate separation. If the humidity of the steam was constant, the capacitance change ratio decreased with an increasing plate separation. (4) The stability of the sensor decreased when the ratio between the plate length and plate separation increased. The linearity of the capacitive sensors increased initially and then decreased when the plate/separation ratio increased.

Acknowledgments

This study was supported by the Doctor Research Foundation at Northeast Dianli University (BSJXM-201306).

References

- [1] Lanford R W, Moore M J. The measurement of steam wetness fraction in operating turbines[C]. Sixth Thermodynamics and Fluid Mechanics Convention, ImechE, 1976, 152.
- [2] Council J R, Ramey H J. Drainage relative permeability obtained from steam-water boiling flow and external gas drive experiments[J]. GRC Transaction, 1979, 3(2): 141-103.
- [3] Luijtana C C M, Dongena M E H, Stormbomb L E. Pressure influence in capacitive humidity measurement[J]. Sensors and Actuators B: Chemical, 1998, 49(7): 279-282.
- [4] Chen J. K, Council J. R. Experimental steam-water permeability curves[J]. GRC Transaction, 1978, 2(1): 102-104.
- [5] Wang Shenglong, Yang Shangrang, Wang Jianguo, etc. Study on a method of wetness measurement on line and industrial test for steam turbine exhaust [J]. Proceedings of the CSEE, 2005, 25(17): 83-87.
- [6] Lovelock B G. Steam flow measurement using alcohol tracers[J]. Geothermics, 2001, 30(6): 641-654.
- [7] Tian Songfeng, Han Zhonghe, Yang Kun. Experiment research on wetness measurement of flowing steam by resonant cavity perturbation[J]. Chinese Journal of Power Engineering, 2005, 25(2): 254-257.
- [8] Ning Deliang. Research on a novel capacitance sensor for measuring wetness of flowing wet steam [D]. Harbin: Harbin Engineering University, 2007.
- [9] Ning Deliang, Yan Changqi, Gao Puzheng. Structure design of novel type capacitance sensor for steam humidity[J]. Transducer and Micro-system Technologies, 2007, 26(3): 65-67.
- [10] Ning Deliang, Pang Fengge, Yan Changqi. Application of a novel instrument for wetness measurement in water-air flows[J]. Journal of Harbin Engineering University, 2006, 27(6): 825-829.
- [11] Kang U, Kensall D. A High-speed capacitive humidity sensor with on-chip thermal reset[J]. IEEE Transactions on Electron Devices, 2000, 147(4): 702-710.
- [12] Gregory, G. A. & Mattar, L. An in-situ volume fraction sensor for two-phase flow of non-electrolytes[R]. J. Can. Pet. Technol, 1973, 12: pp48-52.
- [13] Abouelwafa, M. S. A. & Kendall, E. J. M. Determination of theoretical capacitance of a concave sensor. 1979 Rev. Sci. Instrum. 50: 1158-1159.
- [14] Abouelwafa, M. S. A. & Kendall, E. J. M. The use of capacitance sensors for phase percentage determination in multiphase pipelines[C]. IEEE Tans. Instrum. Measur. 1980, 29: 24-27.
- [15] Borst, J. C. 1983 Een capacitive sensor voor gas-volume fraction metigen[R]. Research Report, Dept of Mechanical Engineering, Delft Univ. of Technology.
- [16] Abdullah A. Kendoush, Zareh A. Sarkis. Improving the accuracy of the capacitance method for void fraction measurement[J]. Experimental Thermal and Fluid Science 1995, 11: 321-326.
- [17] Yu, X., Lu, W., Rong, P., Xu, Q., Chen, D., 2004. Simulation and modeling of square capacitance field sensitivity [C]. 3rd Int. Symp. on Instrument. Sci. and Tech. 18-22.
- [18] Delfo, J.A., Whitaker, S., 2001. Electrohydrodynamics in porous media [J]. Transport in Porous Media. 44, 385-405
- [19] Story P R, Galipeau D W, Mileham R D. A study of low-cost sensors for measuring low relative humidity[J]. Sensors and Actuators B: Chemical, 1995, 25(1-3): 681-685.
- [20] Nahar R K. Study of the performance degradation of thin film aluminum oxide sensors at high humidity[J]. Sensors and Actuators B: Chemical, 2000, 63(1-2): 49-54.

- [21] Dai Chingliang, A capacitive humidity sensor integrated with micro heater and ring oscillator circuit fabricated by CMOS-MEMS technique[J]. *Sensors and Actuators B: Chemical*, 2007, 122(2): 375-380.
- [22] Hsin L C, Hsiu C C. Sensitivity enhancement of capacitive-type photo-resistor-based humidity sensors using deliquescent salt diffusion method[J]. *Sensors and Actuators B: Chemical*, 2008, 129(1): 531-537.
- [23] DU Lipeng, Tian Ruifeng, Zhang Pengfei, Sun Zhongning. Numerical simulation and experiment investigating the performance of a capacitance sensor measuring the humidity of wet steam[J]. *Measurement Science and Technology*. 2011. 11, 22(12).
- [24] Du Lipeng, Tian Ruifeng, Zhang Pengfei, Sun Zhongning. Numerical simulation on coupling performance of steam flow field and electric field in capacitance sensor measuring steam wetness[J]. *Atomic Energy Science and Technology*. 2012. 8, 46(8): 936-942.
- [25] Du Lipeng, Tian Ruifeng, Sun Zhongning, Ning Deliang. Analysis of static response performance of the capacitance sensor measuring the humidity of the wet steam in the air and water system[J]. *Proceeding of CSEE*. 2012. 10, 32 (26) : 86-90.
- [26] Lipeng Du, Ruifeng Tian, Liu Xiaoyi, Sun Zhongning. Numerical simulation and experimental investigation of structural optimization of capacitance sensors for measuring steam wetness with different coaxial cylinders[J]. *Nuclear Engineering and Design*. 2013, 262: 88-97.